Enumeration of Polyominoes & Polycubes Composed of Magnetic Cubes

Yitong Lu[1], Anuruddha Bhattacharjee[2], Daniel Biediger[1], MinJun Kim[2], Aaron T. Becker[1]

***Abstract*— This paper examines a family of designs for magnetic cubes and counts how many configurations are possible for each design as a function of the number of modules. *Magnetic modular cubes* are cubes with magnets arranged on their faces. The magnets are positioned so that each face has either magnetic south or north pole outward. Moreover, we require that the net magnetic moment of the cube passes through the center of opposing faces. These magnetic arrangements enable coupling when cube faces with opposite polarity are brought in close proximity and enable moving the cubes by controlling the orientation of a global magnetic field. This paper investigates the 2D and 3D shapes that can be constructed by magnetic modular cubes, and describes all possible magnet arrangements that obey these rules. We select ten magnetic arrangements and assign a "color" to each of them for ease of visualization and reference. We provide a method to enumerate the number of unique polyominoes and polycubes that can be constructed from a given set of colored cubes. We use this method to enumerate all arrangements for up to 20 modules in 2D and 16 modules in 3D. We provide a motion planner for 2D assembly and through simulations compare which arrangements require fewer movements to generate and which arrangements are more common. Hardware demonstrations explore the self-assembly and disassembly of these modules in 2D and 3D.**

I. Introduction

Large groups of small-scale modular robots are often designed to be externally manipulated. Magnetic forces are a popular choice for manipulating these robots because the robots can be directly controlled simply by incorporating magnets or ferromagnetic material in the robot body. In the last few decades, many research projects have been conducted based on magnetic actuation and coupling systems to explore reconfigurable modular robotics at different length scales [1]–[4]. Much related work has focused on the "Tilt model" where components move in a straight line until they hit an obstacle, and combine when mating particles are brought close together. Solutions often design workspace obstacles that enable arbitrary reconfiguration of components pushed by a global force [5], [6]. We designed algorithms that enabled efficient construction of desired shapes [7], and workspace obstacles that enabled sorting and classifying constructed polyominoes [8]. This previous work did not consider the stability or robustness of the structures generated. Recent work in [9], [10] examined the forces between individual components and evaluated if a structure of module robots would be stable — if it would topple or

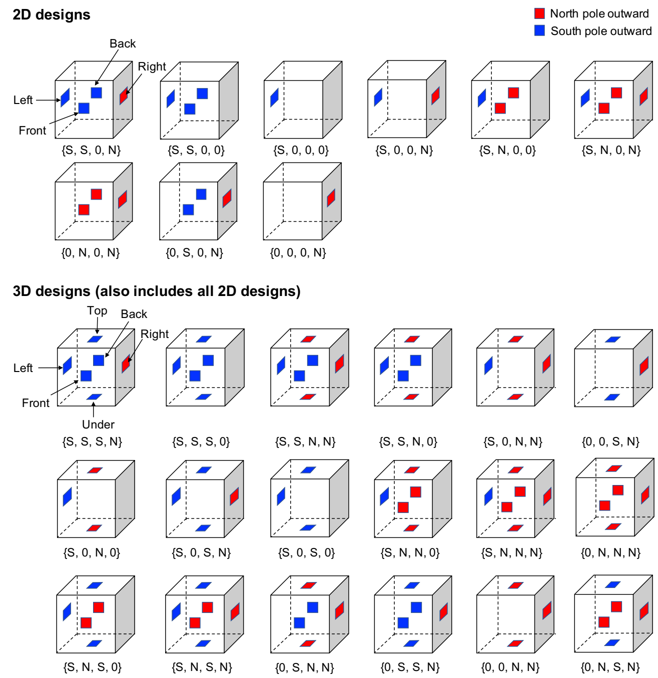

Fig. 1. Designs of 2D and 3D modular cubes. Underneath each cube the arrangement is labeled as {left [L], front [F]/back [B], top [T]/under [U], right [R]}.

collapse under its own weight, especially during the process of reconfiguration.

Our future goal is to design motion plans for magnetic modular cubes to enable them to form shapes suitable for fast motion, yet with designed fracture points so they can be easily disassembled at a goal and reconfigured into tools or structures. As first steps toward that goal, this paper presents the following contributions: (1) Design and demonstrations of magnetic modular cubes (MMCs) which are simple in design, scalable, and highly reconfigurable through controlled assembly-disassembly. (2) Analysis of all possible magnetization profiles that match the specifications of our modular cubes. (3) A method to count the number of unique configurations for a given set of cubes. (4) Enumerate the unique configurations up to $n = 20$ in 2D and $n = 16$ in 3D. (5) Provide a motion planner for 2D assembly. (6) Monte Carlo simulations to measure the frequency that certain shapes can be constructed and the required number of movement steps to generate the shapes. (7) Conduct hardware experiments that explore the self-assembly and disassembly of these modules in 2D and 3D. For applications of these magnetic cubes, see [11]. For a lengthened version of this paper, see [12].

This work used HPE DSI/IT computational resources and was supported by the NSF under Grant Nos. [IIS-1553063, IIS-1849303, CNS-1932572] .

[1]Authors are with the University of Houston, Houston, TX 77204 USA {ylu36, debiediger, atbecker}@uh.edu.

[2]Authors are with Southern Methodist University, Dallas, TX 75275 USA {abhattacharjee, mjkim}@lyle.smu.edu.

II. Design of Magnetic Modular Cubes

We design the MMCs so they can be controlled by a global magnetic field. The cubes are manufactured so they align with an applied magnetic field. The global magnetic field provides a reference frame with a magnetic south to the left and north to the right. We labeled each face of the cube as [L, F, B, T, U, R] for *left*, *front*, *back*, *top*, *under*, and *right* faces. On each face at most one axially magnetized permanent magnet is embedded. Each cube must have a net magnetic orientation. The magnets are positioned with poles facing outwards such that each face is either north or south and such that the net magnetic moment of the cube from magnetic south to north passes through the center of opposing faces (see Fig. 1). This net magnetic moment is required because it enables "pivot walking" and "rolling" the cubes. Pivot walking is a movement gait that alternately lifts the north or south pole of the cube so the cube balances on the opposing edge, and then applies torque to spin the cube on the balancing edge, as in [11], [13], [14]. The rolling motion [15] can be achieved by applying continuous rotational magnetic torque along an axis perpendicular to the axis of net magnetization of a cube.

Due to the MMCs' cubic design, magnetically connected structures of MMCs are polyominoes in 2D and polycubes in 3D. Polyominoes and polycubes are a classic topic in combinatorics. Related work on enumerating polyominoes and polycubes include [16]–[20] and coloring them [21]. Work on upper and lower bounds for the number of polyominoes and polycubes is an active research area [20], [22], and will be relevant to modular robotic construction.

Similarly, there has been a great deal of recent research on how to design workspaces that exploit global control of magnetic particles to design arbitrary shapes [6], [23], [24], and on the complexity of motion planning under such constraints. These papers provide important solutions on how to design workspaces that enable fast rearrangement of cubes, but they do not provide insight on how to build those cubes. Moreover, these works tend to assume all cubes will stick together if brought close enough in proximity. In contrast, this paper focuses on the configurations made possible by the magnetic profiles of the cubes.

III. Generate all possible polyominoes in 2D

Polyominoes are face-connected sets of unit cubes that lie on the square-grid graph. Each cube is represented by an integer tuple (x, y). Cubes (x_1, y_1) and (x_2, y_2) are adjacent if $|x_1 - x_2| + |y_1 - y_2| = 1$. Two *free polyominoes* are considered distinct if they have different shapes, but they cannot be rotations of each other. Two *fixed polyominoes* are considered distinct if they have different shapes or orientations. Because the global magnetic field provides an orientation, we consider fixed polyominoes for our MMCs design. The number of fixed polyominoes of size n is denoted by $A_{n,\text{2D}}$. The number of polyominoes grows exponentially [22]

$$\lim_{n \to \infty} (A_{n,\text{2D}})^{\frac{1}{n}} = \lambda. \quad (1)$$

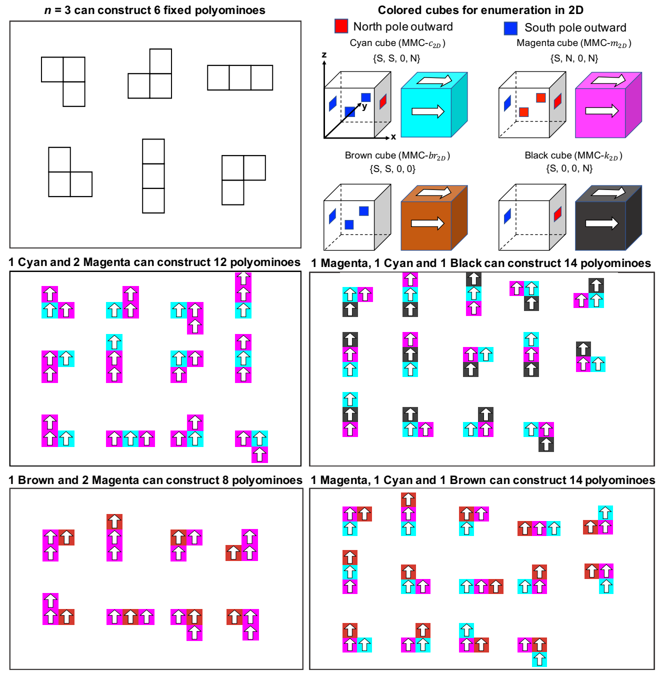

Fig. 2. Enumeration of colored cubes in 2D. The composition of cube types determines the number of polyominoes that can be made. The white arrow indicates the direction of south to north magnetic pole.

We implemented a method to enumerate the fixed polyominoes and unique colored polyominoes that can be constructed by a set of MMCs [25]. Based on the hardware experiment environment (see Section V), we developed a 2D motion planner using a bounded 11×11 workspace that generates the set of valid colored polyominoes reachable by global moves from an initial configuration. We select four magnet arrangements that use at least two magnets and, for ease of visualization, assign them the colors cyan, magenta, brown, and black (see Fig. 2 top right).

A. Enumeration of fixed polyominoes

To enumerate fixed polyominoes, we implemented the method used by Redelmeier in [26]. We use a variant of this algorithm to enumerate colored polyominoes constructed from MMCs. Because the magnets in these cubes define a coordinate system, we enumerate all polyominoes with magnetic moments pointing in the $+y$ direction. The algorithm works by recursively generating all cubes up to a given size n. We start with the leftmost cube of the bottom row, placed at the origin $(0, 0)$. For a given configuration with k cubes, the algorithm generates a new configuration of size $k + 1$ by adding a cube connected to the polyomino. We maintain a list of the adjacent cubes, *list_adj*, and a list of which adjacent cubes have been selected, *poly*, for each recursive call. In the initial call, the list of adjacent cubes, *list_adj*, consists of the origin $(0, 0)$, the cube above the origin $(0, 1)$, and the cube to the right of the origin $(1, 0)$. We set *poly*[0] = 0. At each recursive call, if $k \equiv n$, the procedure returns. Otherwise, a recursive call is made for each cube in *list_adj* greater than the last cube in *poly*. For each of these calls, the cube is added to *poly*, and any cubes adjacent to the new cube are appended to *list_adj* if they are

TABLE I. NUMBER OF FIXED POLYOMINOES $A_{n,2D}$, WHERE n IS THE NUMBER OF CUBES. WITH MMC-M_{2D} AND MMC-C_{2D}, $C_{n,i}$ IS THE NUMBER OF COLORED POLYOMINOES WITH i MAGENTA CUBES AND n TOTAL CUBES. ROW MAXIMUM IN ORANGE.

n	$A_{n,2D}(n)$	$C_{n,0}$ (with 0 magenta cubes)	$C_{n,1}$ (with 1 magenta cube)	$C_{n,2}$ (with 2 magenta cubes)	$C_{n,3}$ (with 3 magenta cubes)	$C_{n,4}$ (with 4 magenta cubes)	$C_{n,5}$ (with 5 magenta cubes)	$C_{n,6}$ (with 6 magenta cubes)	$C_{n,7}$ (with 7 magenta cubes)	$C_{n,8}$ (with 8 magenta cubes)	$C_{n,9}$ (with 9 magenta cubes)	$C_{n,10}$ (with 10 magenta cubes)
1	1	1	1									
2	2	1	4	1								
3	6	1	12	12	1							
4	19	1	26	64	26	1						
5	63	1	46	230	230	46	1					
6	216	1	72	642	1,256	642	72	1				
7	760	1	105	1,505	5,070	5,070	1,505	105	1			
8	2,725	1	146	3,107	16,542	28,166	16,542	3,107	146	1		
9	9,910	1	196	5,828	45,992	122,248	122,248	45,992	5,828	196	1	
10	36,446	1	256	10,163	112,934	440,761	684,848	440,761	112,934	10,163	256	1
11	135,268	1	327	16,745	251,269	1,374,201	3,116,870	3,116,870	1,374,201	251,269	16,745	327
12	505,861	1	410	26,373	516,274	3,810,917	12,049,830	17,549,004	12,049,830	3,810,917	516,274	26,373
13	1,903,890	1	506	40,038	993,922	9,598,673	40,816,089	82,606,576	82,606,576	40,816,089	9,598,673	993,922
14	7,204,874	1	616	58,955	1,813,104	22,313,159	123,919,688	336,242,252	466,659,024	336,242,252	123,919,688	22,313,159
15	27,394,666	1	741	84,595	3,161,438	48,479,302	343,116,501	1,212,929,807	2,252,676,080	2,252,676,080	1,212,929,807	343,116,501
16	104,592,937	1	882	118,721	5,305,344	99,443,287	878,332,642	3,950,577,893	9,540,203,060	12,756,460,434	9,540,203,060	3,950,577,893
17	400,795,844	1	1,040	163,426	8,615,301	194,158,877	2,101,617,914	11,788,730,647	36,159,880,264	62,793,912,275	62,793,912,275	36,159,880,264
18	1,540,820,542	1	1,216	221,173	13,597,154	363,234,599	4,742,584,436	32,609,407,748	124,582,102,308	274,438,170,936	356,238,273,248	274,438,170,936
19	5,940,738,676	1	1,411	294,839	20,930,653	654,689,624	10,168,537,421	84,420,978,408	395,042,625,208	1,082,576,666,561	1,781,181,487,071	1,781,181,487,071
20	22,964,779,660	1	1,626	387,759	31,516,302	1,141,991,891	20,843,326,708	206,179,417,105	1,164,668,766,352	3,905,398,277,399	7,986,377,556,212	10,119,349,228,496

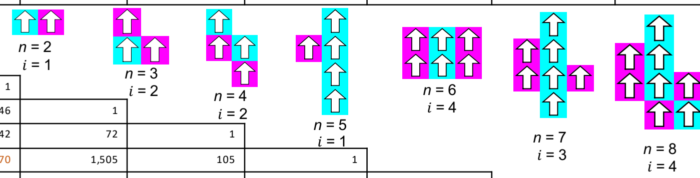

not already in *list_adj*. To avoid generating the same cube more than once, cubes are only added if they are above the origin, or in the same row to the right of the origin: $\{(x, y) \mid (y > 0) \text{ or } (y \equiv 0 \text{ and } x \geq 0)\}$.

B. Enumeration of valid colored polyominoes from a set

To count the number of valid colored polyominoes from a set of colored cubes, we modify the previous algorithm. We include the coloring information in *poly*. Before each recursive call, we check if the new cube can be colored in the given color. A check is successful if there are sufficient unused cubes of the color, and if placing the cube does not violate any of the magnetic-assembly rules. If the check is successful, a recursive call is performed. Fig. 2 top left shows that for $n = 3$ cubes, 6 fixed polyominoes can be enumerated. Using a supply with one cyan and two magenta cubes produces more polyominoes than one brown and two magenta cubes. However, using three colored cubes enables constructing even more colored polyominoes.

Table I shows the number of fixed polyominoes that can be enumerated with up to $n = 20$ cubes. It also lists the number of valid polyominoes with magenta and cyan cubes that can be constructed by coloring them with up to 20 cyan cubes. With zero to two magenta cubes, the number of valid polyominoes is less than the number of fixed polyominoes ($C_{n,i}$ for i = 0, 1 or 2). This is because two magenta or two cyan cubes can only be connected in series (with arrows aligned tip-to-tail). However, a more extensive set of polyominoes with different shapes and orientations can be constructed when the fraction of magenta cubes is increased. The largest variety is possible when $i = \lfloor \frac{n}{2} \rfloor$.

C. Self-assembly algorithm

We provide a low-fidelity motion model that can compute reachable polyomino configurations and the shortest movement sequences for a set of MMCs from an initial configuration. We assume that all modules move at the same speed in the same direction, unless they encounter a fixed obstacle. Without loss of generality, we limit the movement directions to north, east, south, and west.

Fig. 3 shows an example of all the valid colored polyominoes can be generated with 4 different cube designs. The initial configuration and the details of the movements are shown on the right. Underneath each polyomino is listed the shortest step sequence to construct it. At each step, we could move one unit length in the four cardinal directions {n, e, s, w} or rotate {r} counterclockwise (CCW) or clockwise (CW) a quarter-turn. We prune this search by only allowing rotations if no translation moves have been made and by only performing CW rotations. For example, in this shorthand, "2r, 4w, 6n" means rotate 180° CW followed by four unit moves west, and then six unit moves north. We used a breadth-first search (BFS) algorithm to discover these reachable configurations. The root of the search is the initial configuration, and we maintain a list of all relative configurations that have been reached. A *relative configuration* is represented by rotating the coordinate frame so that the magnetic north points up and then translating all cubes. To further prune the tree, we only switch direction if the relative configuration of the cubes changes, and we terminate search branches if the present configuration has occurred before. When the relative configuration changes, we call this an *intermediate configuration*. Intermediate configurations occur when at least one cube (but not all cubes) strikes an obstacle. When this occurs, the new relative configuration is compared to the list and is only appended if it is unique. After the polyomino is assembled, we compare the paths taken to save the shortest step sequence to construct the structure.

IV. GENERATE ALL POSSIBLE POLYCUBES IN 3D

A *polycube* is a three-dimensional polyomino constructed by cubes attaching face to face. Each cube is represented by an integer tuple (x, y, z). Cubes 1 and 2 are adjacent if $|x_1 - x_2| + |y_1 - y_2| + |z_1 - z_2| = 1$. Polycubes can be enumerated in two ways, depending on whether different orientations are counted as one polycube or two. Two *free polycubes*

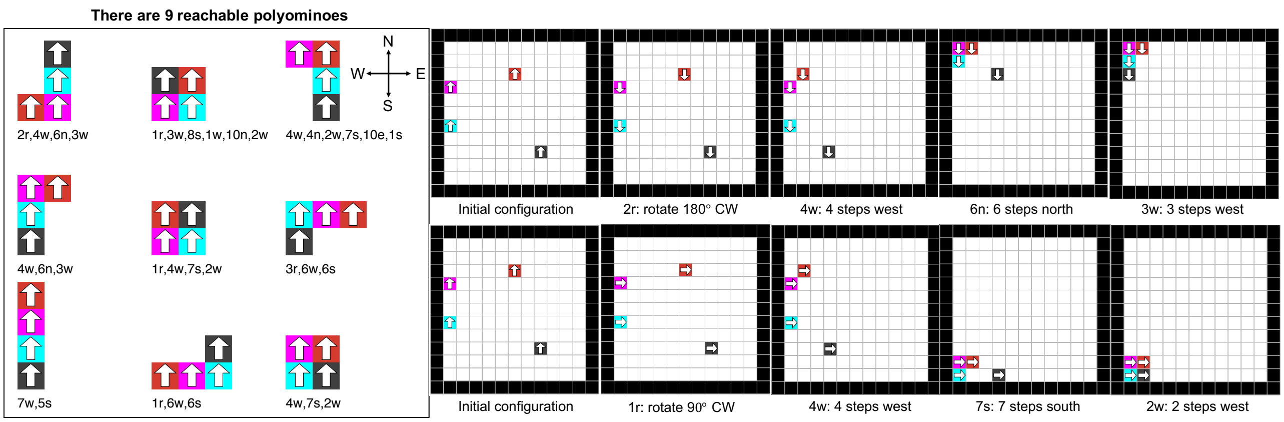

Fig. 3. **Left**: The self-assembly result for an arbitrary initial configuration of four cubes with different designs. **Right**: Details of the movements.

TABLE II. NUMBER OF FIXED POLYCUBES $A_{n,3D}$, WHERE n IS THE NUMBER OF CUBES. ROW MAXIMUM IN ORANGE. WITH MMC-R$_{3D}$ AND MMC-B$_{3D}$, $C_{n,i}$ IS THE NUMBER OF COLORED POLYCUBES WITH i RED CUBES AND n TOTAL CUBES.

n	$A_3(n)$	$C_{n,0}$ (with 0 red cubes)	$C_{n,1}$ (with 1 red cube)	$C_{n,2}$ (with 2 red cubes)	$C_{n,3}$ (with 3 red cubes)	$C_{n,4}$ (with 4 red cubes)	$C_{n,5}$ (with 5 red cubes)	$C_{n,6}$ (with 6 red cubes)	$C_{n,7}$ (with 7 red cubes)	$C_{n,8}$ (with 8 red cubes)
1	1	1	1							
2	3	1	6	1						
3	15	1	25	25	1					
4	86	1	76	228	76	1				
5	534	1	188	1,322	1,322	188	1			
6	3,481	1	404	5,745	12,764	5,745	404	1		
7	23,502	1	794	20,407	86,394	86,394	20,407	794	1	
8	162,913	1	1,472	62,532	456,712	855,148	456,712	62,532	1,472	1
9	1,152,870	1	2,614	171,452	2,008,012	6,349,175	6,349,175	2,008,012	171,452	2,614
10	8,294,738	1	4,482	431,506	7,651,944	38,050,258	63,779,954	38,050,258	7,651,944	431,506
11	60,494,549	1	7,456	1,015,046	26,019,733	192,891,333	503,439,919	503,439,919	192,891,333	26,019,733
12	446,205,905	1	12,074	2,260,876	80,665,094	854,490,806	3,291,665,860	5,106,180,788	3,291,665,860	854,490,806
13	3,322,769,321	1	19,081	4,813,494	231,730,812	3,387,693,736	18,482,785,142	42,090,555,948	42,090,555,948	18,482,785,142
14	24,946,773,111	1	29,488	9,864,029	624,652,660	12,240,460,603	91,492,419,452	293,391,588,337	429,795,275,568	293,391,588,337
15	188,625,900,446	1	44,642	19,557,394	1,595,479,330	40,884,804,683	407,278,041,600	1,779,496,771,333	3,659,031,289,311	3,659,031,289,311
16	1,435,074,454,755	1	66,308	37,665,527	3,891,150,962	127,677,329,720	1,655,859,431,014	9,595,622,196,073	26,786,720,783,388	37,549,711,897,172

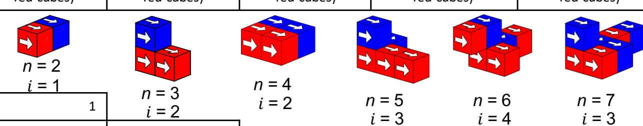

are considered distinct if they have different shapes, but are not 3D rotations of each other. Two *fixed polycubes* are considered equivalent if one can be transformed into the other by a translation. The number of fixed three-dimensional polycubes of size n is denoted by $A_{n,3D}$.

A. Enumeration of valid colored polycubes from a set

We select six magnet arrangements that use at least four magnets and assign them the colors in Fig. 5 top right. As with the enumeration of valid colored polyominoes in 2D, to count the number of valid colored polycubes generated from a set of MMCs, we color the cubes while enumerating fixed polycubes during the recursive step. Fig. 5 top left shows that for $n = 3$ cubes, 15 fixed polycubes can be enumerated. Middle left and bottom left figures show examples of coloring with two colors. Using a supply with red and blue cubes can produce more polycubes than red and green. With a supply of three colors, a wider variety of valid colored polycubes can be constructed.

Table II shows the number of fixed polycubes that can be enumerated with up to $n = 16$ cubes and the number of valid polycubes that can be constructed by coloring them with red and blue cubes. The top right corner of the table shows examples of valid colored polycubes. Fig. 4 left shows the maximum number of valid polycubes that can be constructed with five different sets of cubes in 3D, where n is the total number of cubes. For each cube set, the left column shows the maximum number of valid colored polycubes that can be generated for a given total number of cubes. The right column in each set (gray font) shows configurations in a shorthand, e.g. "1r4b" means 1 red and 4 blue cubes.

B. Rejecting non-magnetically connected components

Our enumeration of valid polyominoes (or polycubes) allows placing a cube face without magnets next to a cube of any color, but there is no magnetic connection. Our goal for the polyominoes (or polycubes) is to create aggregates that can be manipulated in unison by a magnetic field. For the purpose of this study, we require that every cube be magnetically connected to form a single component. This requires connected-component analysis. Connected-component labelling is normally used for distinguishing different objects in a binary image [27]. A *magnetically-connected component* is a set of cubes, C, such that for any two cubes in C, there is a valid connected path between them and this path is contained in C. A *valid connection* between two MMCs means the two cubes share a face and on this face one cube has a south pole outward and the other has a

n	all red		red & blue		red & green		red & blue & purple		red & blue & green	
1	1	1r								
2	1	2r	6	1r1b	4	1r1g				
3	1	3r	25	2r1b / 1r2b	12	2r1g / 1r2g	36	1r1b1c	54	1r1b1g
4	1	4r	228	2r2b	64	2r2g	274	2r1b1c	354	2r1b1g / 1r2b1g
5	1	5r	1,322	2r3b / 3r2b	230	2r3g / 3r2g	2,700	2r2b1c	4,227	2r2b1g
6	1	6r	12,764	3r3b	1,256	3r3g	23,184	3r2b1c	31,404	3r2b1g / 2r3b1g
7	1	7r	86,394	3r4b / 4r3b	5,070	3r4g / 4r3g	231,650	3r3b1c	359,982	3r3b1g
8	1	8r	855,148	4r4b	28,166	4r4g	2,090,392	4r3b1c	2,890,392	4r3b1g / 3r4b1g
9	1	9r	6,349,175	4r5b / 5r4b	122,248	4r5g / 5r4g	21,062,329	4r4b1c	32,511,445	4r4b1g
10	1	10r	63,779,954	5r5b	684,848	5r5g	180,597,736	5r4b1c	274,733,776	5r4b1g / 4r5b1g

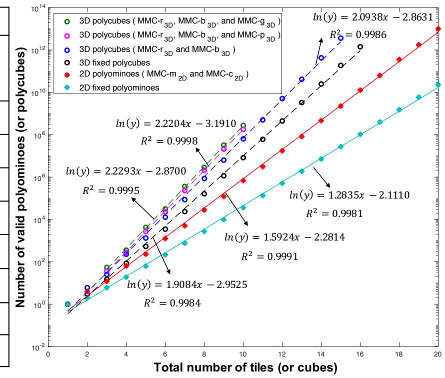

Fig. 4. **Left**: Maximum number of valid colored 3D polycubes with different sets of cube colors, where n is the total number of cubes. **Right**: Enumeration results of valid colored polyominoes and polycubes.

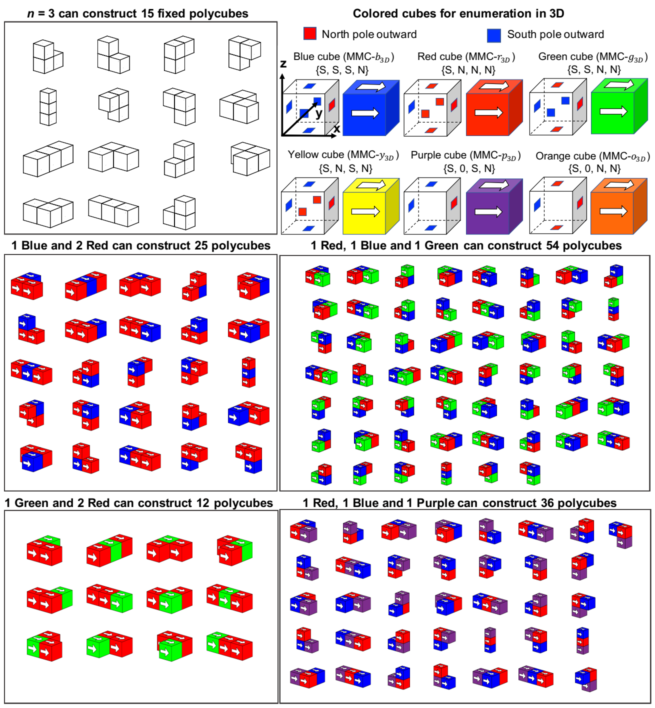

Fig. 5. Enumeration of colored cubes in 3D. The composition of cube types determines the number of polycubes that can be made. The white arrow indicates the direction of south to north magnetic pole.

north pole outward. Before adding a polycube of size n to our enumeration, we first check that the polycube is a single magnetically-connected component. We start with the $(0, 0, 0)$ cube, and perform a breadth-first search on all valid-connected neighboring cubes. The polycube is only counted if the number of connected cubes is n.

C. Time complexity

As with the enumeration scheme by Redelmeier, our enumeration counts each possible polyomino and polycube only one time, the enumeration complexity is exponential, $O(c_{\text{2D}}^n)$ and $O(c_{\text{3D}}^n)$. Our implementation is slightly less efficient if we allow cubes that do not have magnets on each side, since we generate intermediate configurations that might not form a magnetically-connected component. After constructions, the final step is to check if the polycube is magnetically-connected, and reject those that are not. The connected check requires $O(n)$ time. 3D construction is more complex than 2D, so the constant $c_{\text{3D}} > c_{\text{2D}}$. Fig. 4 right shows the results of enumeration of valid colored polyominoes and polycubes.

V. Experimental Setup and Results

A large-scale nested triaxial Helmholtz coil system was used to conduct experiments. The 3D magnetic field vector produced from the system is represented by

$$\boldsymbol{B} = \begin{bmatrix} B_x \\ B_y \\ B_z \end{bmatrix} = \begin{bmatrix} A\cos(\alpha)\cos(\theta) \\ A\cos(\alpha)\sin(\theta) \\ A\sin(\alpha) \end{bmatrix}, \quad (2)$$

where $\boldsymbol{B}$ is the applied magnetic flux density, B_x, B_y, and B_z are the three-dimensional components along x, y and z-axes respectively, A is the amplitude, α is the pitch angle, and θ is the yaw angle. Each cube has a volume of 1cm^3.

A magnetic flux of 10mT was enough to actuate the modular cubes and achieve successful assembly. Pivot walking motion was used to actuate individual modular cubes with precise motion, following predetermined paths to create a target assembly. When the arrows on top faces of the modular cubes are aligned side-by-side, this is defined as a parallel assembly. When the arrows are aligned tip-to-tail, this is defined as a serial assembly. The self-assembly is caused by the magnetic attraction force generated from embedded permanent magnets in the modular cubes when they are moved close to each other.

Fig. 6 shows a representative 3D construction sequence using global magnetic control. A 3D self-assembly was performed following a 2D self-assembly to create a pair of sub-assemblies. The process formed an ⅃-shape and a square-shape with different cube orderings at 36s. The sub-assemblies were rotated CW (at 30s) and CCW (at 47s) for movement in different directions. Once 2D structures were formed with pivot walking motion followed by 2D self-assembly, the sub-units can be further joined in 3D by using rolling motions. The rolling motion was achieved by applying continuous rotational magnetic torque on the modular structures about a fixed axis until the target location was reached (from 57s to 66s). While the sub-assemblies were rolled to bring them in close proximity, a blue modular cube in the ⅃-shaped structure was disassembled (at 65s). The blue cube reattached to the square-shaped structure (at

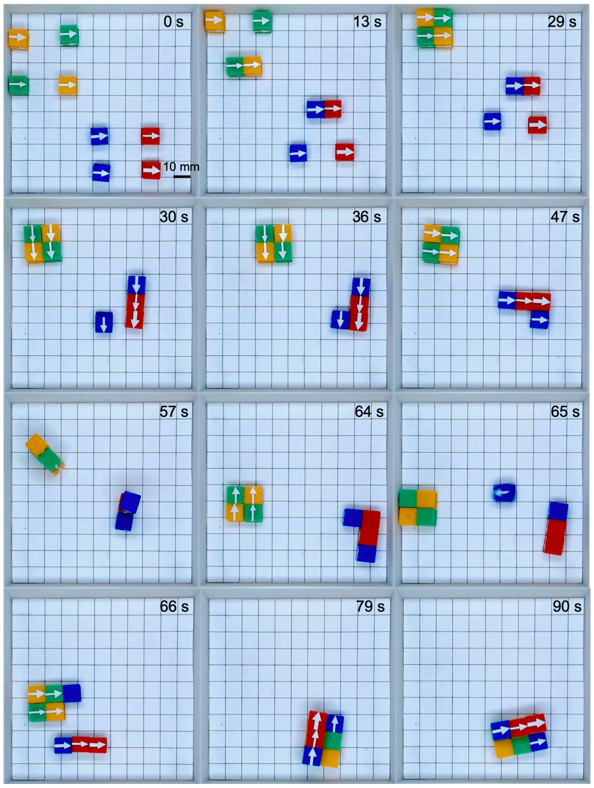

Fig. 6. 3D self-assembly and disassembly behavior with eight cubes.

66s) which resulted in an unplanned reconfiguration. This spontaneous disassembly and reconfiguration could have benefits, but could also be avoided with improved control. Once the reconfigured sub-units move into close proximity, they self-assembled to create a two layered 3D structure (at 79s). This 3D structure was also actuated in the workspace with the pivot walking motion (from 79s to 90s).

VI. Future Work

Future work will focus on 3D planning, in particular making a high-fidelity simulator for motion planning. It would be interesting to calculate the number of valid colorings of a given polycube as a function of the supply of colored cubes. During the enumeration process one could also catalog useful configurations, ranking them on their mechanical stability, fracture modes, or magnetic profile in addition to their shape.

References

[1] J. W. Romanishin, K. Gilpin, and D. Rus, "M-blocks: Momentum-driven, magnetic modular robots," in *IROS*. IEEE, 2013, pp. 4288–4295.

[2] S. Tasoglu, C. Yu, H. Gungordu, S. Guven, T. Vural, and U. Demirci, "Guided and magnetic self-assembly of tunable magnetoceptive gels," *Nature Communications*, vol. 5, no. 1, pp. 1–11, 2014.

[3] H. Xie, M. Sun, X. Fan, Z. Lin, W. Chen, L. Wang, L. Dong, and Q. He, "Reconfigurable magnetic microrobot swarm: Multimode transformation, locomotion, and manipulation," *Science Robotics*, vol. 4, no. 28, 2019.

[4] W. Saab, P. Racioppo, and P. Ben-Tzvi, "A review of coupling mechanism designs for modular reconfigurable robots." *Robotica*, vol. 37, no. 2, pp. 378–403, 2019.

[5] J. Balanza-Martinez, A. Luchsinger, D. Caballero, R. Reyes, A. A. Cantu, R. Schweller, L. A. Garcia, and T. Wylie, "Full tilt: Universal constructors for general shapes with uniform external forces," in *Proceedings of the Thirtieth Annual ACM-SIAM Symposium on Discrete Algorithms*. SIAM, 2019, pp. 2689–2708.

[6] J. Balanza-Martinez, T. Gomez, D. Caballero, A. Luchsinger, A. A. Cantu, R. Reyes, M. Flores, R. Schweller, and T. Wylie, "Hierarchical shape construction and complexity for slidable polyominoes under uniform external forces," in *Symposium on Discrete Algorithms*. SIAM, 2020, pp. 2625–2641.

[7] A. T. Becker, S. P. Fekete, P. Keldenich, D. Krupke, C. Rieck, C. Scheffer, and A. Schmidt, "Tilt assembly: Algorithms for micro-factories that build objects with uniform external forces," *Algorithmica*, vol. 82, no. 2, pp. 165–187, 2020.

[8] P. Keldenich, S. Manzoor, L. Huang, D. Krupke, A. Schmidt, S. P. Fekete, and A. T. Becker, "On designing 2d discrete workspaces to sort or classify polynminoes," in *IROS*. IEEE, 2018, pp. 1–9.

[9] P. Hołobut and J. Lengiewicz, "Distributed computation of forces in modular-robotic ensembles as part of reconfiguration planning," in *2017 IEEE International Conference on Robotics and Automation (ICRA)*. IEEE, 2017, pp. 2103–2109.

[10] B. Piranda, P. Chodkiewicz, P. Hołobut, S. Bordas, J. Bourgeois, and J. Lengiewicz, "Distributed prediction of unsafe reconfiguration scenarios of modular-robotic programmable matter," *preprint arXiv:2006.11071*, 2020.

[11] A. Bhattacharjee, Y. Lu, A. T. Becker, and M. Kim, "Magnetically-controlled modular cubes with reconfigurable self-assembly and disassembly," *IEEE Transactions on Robotics*, 2021.

[12] Y. Lu, A. Bhattacharjee, D. Biediger, M. Kim, and A. T. Becker, "Enumeration of polyominoes & polycubes composed of magnetic cubes," in *ArXiv*, July 2021. [Online]. Available: https://arxiv.org/abs/2107.10167

[13] E. Al Khatib, A. Bhattacharjee, P. Razzaghi, L. W. Rogowski, M. J. Kim, and Y. Hurmuzlu, "Magnetically actuated simple millirobots for complex navigation and modular assembly," *IEEE Robotics and Automation Letters*, vol. 5, no. 2, pp. 2958–2965, 2020.

[14] L. Rogowski, A. Bhattacharjee, X. Zhang, G. Kararsiz, H. Fu, and M. J. Kim, "Manipulation planning of magnetically actuated programmable cuboids for collaborative assembly," in *2020 IEEE/RSJ International Conference on Intelligent Robots and Systems, Las Vegas, NV, USA*, 2020.

[15] C. Bi, M. Guix, B. V. Johnson, W. Jing, and D. J. Cappelleri, "Design of microscale magnetic tumbling robots for locomotion in multiple environments and complex terrains," *Micromachines*, vol. 9, no. 2, p. 68, 2018.

[16] G. Aleksandrowicz and G. Barequet, "Counting d-dimensional polycubes and nonrectangular planar polyominoes," in *International Computing and Combinatorics Conference*. Springer, 2006, pp. 418–427.

[17] S. Luther and S. Mertens, "Counting lattice animals in high dimensions," *Journal of Statistical Mechanics: Theory and Experiment*, vol. 2011, no. 09, p. P09026, 2011.

[18] G. Barequet and M. Shalah, "Polyominoes on twisted cylinders," in *Proceedings of the Twenty-Ninth Annual Symposium on Computational Geometry*, 2013, pp. 339–340.

[19] A. R. Conway, "The design of efficient algorithms for enumeration," *preprint arXiv:1610.09806*, 2016.

[20] G. Barequet and M. Shalah, "Improved upper bounds on the growth constants of polyominoes and polycubes," *preprint arXiv:1906.11447*, 2019.

[21] E. D. Demaine, M. L. Demaine, D. Eppstein, and J. O'Rourke, "Some polycubes have no edge-unzipping," *preprint arXiv:1907.08433*, 2019.

[22] G. Barequet, G. Rote, and M. Shalah, "$\lambda > 4$: An improved lower bound on the growth constant of polyominoes," *Commun. ACM*, vol. 59, no. 7, pp. 88–95, 2016.

[23] D. Caballero, A. A. Cantu, T. Gomez, A. Luchsinger, R. Schweller, and T. Wylie, "Building patterned shapes in robot swarms with uniform control signals," in *Proceedings of CCCG*, 2020.

[24] U. K. Cheang, F. Meshkati, H. Kim, K. Lee, H. C. Fu, and M. J. Kim, "Versatile microrobotics using simple modular subunits," *Scientific Reports*, vol. 6, p. 30472, 2016.

[25] Y. Lu and A. T. Becker, March 2021. [Online]. Available: https://github.com/RoboticSwarmControl/EnumeratingPolycubes/

[26] D. H. Redelmeier, "Counting polyominoes: yet another attack," *Discrete Math.*, vol. 36, no. 2, pp. 191–203, 1981.

[27] L. He, X. Ren, Q. Gao, X. Zhao, B. Yao, and Y. Chao, "The connected-component labeling problem: A review of state-of-the-art algorithms," *Pattern Recognition*, vol. 70, pp. 25–43, 2017.